STUDY ON ANOMALOUS NEUTRAL TRIPLE-GAUGE BOSON COUPLINGS FROM DIMENSION-EIGHT OPERATORS AT THE HL-LHC*

A. Senol, H. Denizli

Department of Physics, Bolu Abant Izzet Baysal University, 14280 Bolu, Turkey
senol_a@ibu.edu.tr
denizli_h@ibu.edu.tr

A. Yilmaz

Department of Electrical and Electronics Engineering, Giresun University
28200 Giresun, Turkey
aliyilmaz@giresun.edu.tr

I. Turk Cakir

Department of Energy Systems Engineering, Giresun University
28200 Giresun, Turkey
ilkay.turk.cakir@cern.ch

O. Cakir

Department of Physics, Ankara University, 06100 Ankara, Turkey
ocakir@science.ankara.edu.tr

(Received August 21, 2019; accepted October 11, 2019)

The anomalous neutral triple-gauge boson couplings (aNTGCs) for the $Z\gamma\gamma$ and $Z\gamma Z$ vertices described by dimension-eight operators are examined through the process $pp \to l^+l^-\gamma$ at High-Luminosity Large Hadron Collider (HL-LHC). We performed an analysis on transverse momentum of photon and angular distribution of charged lepton in the final state including detector effects. Sensitivity limits of the $C_{\tilde{B}W}$, C_{BB} couplings are obtained at 95% C.L. to constrain for the ranges $[-1.88; 1.88]$ TeV^{-4}, $[-1.47 : 1.47]$ TeV^{-4} and $[-1.14 : 1.14]$ TeV^{-4}, $[-0.86; 0.86]$ TeV^{-4} with an integrated luminosity of 300 fb^{-1} and 3000 fb^{-1}, respectively.

DOI:10.5506/APhysPolB.50.1597

1. Introduction

The Standard Model (SM) through the non-Abelian $\mathrm{SU(2)_L} \times \mathrm{U(1)}_Y$ gauge group of the electroweak sector predicts the gauge boson self-interactions. The tree-level vertices of three neutral gauge bosons are not allowed since they violate the underlying $\mathrm{SU(2)_L} \times \mathrm{U(1)}_Y$ symmetry. Deviations of triple gauge couplings from SM expectations can provide clues about the new physics beyond the SM. The effect of new physics can be parametrized in a model-independent way by an effective Lagrangian at TeV energy scale. Using effective field theory (EFT), the Lagrangian for neutral triple gauge boson interactions can be written as [1]

$$\mathcal{L}^{\mathrm{nTGC}} = \mathcal{L}^{\mathrm{SM}} + \sum_i \frac{C_i}{\Lambda^4} \left(\mathcal{O}_i + \mathcal{O}_i^\dagger \right) , \tag{1}$$

where Λ is the new physics scale, i runs over the label of four operators expressed as

$$\mathcal{O}_{BW} = iH^\dagger B_{\mu\nu} W^{\mu\rho} \{D_\rho, D^\nu\} H , \tag{2}$$

$$\mathcal{O}_{WW} = iH^\dagger W_{\mu\nu} W^{\mu\rho} \{D_\rho, D^\nu\} H , \tag{3}$$

$$\mathcal{O}_{BB} = iH^\dagger B_{\mu\nu} B^{\mu\rho} \{D_\rho, D^\nu\} H , \tag{4}$$

$$\mathcal{O}_{\tilde{B}W} = iH^\dagger \tilde{B}_{\mu\nu} W^{\mu\rho} \{D_\rho, D^\nu\} H , \tag{5}$$

where $\tilde{B}_{\mu\nu}$ is the B-field strength tensor.

The coefficients $C_{\tilde{B}W}$ (CP conserving) and C_{BB}, C_{BW}, C_{WW} (CP violating) of dimension-eight operators describe anomalous Neutral Triple Gauge Couplings (aNTGC). The contributions from new physics is expected to be suppressed by the inverse powers of the scale of new physics. When the new physics appears at the high-energy scale, the largest contribution to the subprocess $q\bar{q} \to Z\gamma$ is expected from the interference between the SM and the dimension-eight operators. The resulting matrix-element squared for the process $pp \to Z\gamma$ (where $Z \to l^+ l^-$ with $l^\pm = e^\pm, \mu^\pm$) is given by

$$|M|^2 = |M_{\mathrm{SM}}|^2 + 2\mathrm{Re}\left(M_{\mathrm{SM}} M_{\mathrm{D8}}^*\right) + |M_{\mathrm{D8}}|^2 . \tag{6}$$

Here, the last term could be small due to the factor $\sim C_i^2 \Lambda^{-8}$ when the Λ is kept as high-energy scale. However, second term may contribute importantly since the interference takes contribution proportional to $\sim C_i \Lambda^{-4}$. The total cross section for $pp \to l^+ l^- \gamma$ process can be written as $\sigma_{\mathrm{tot}} = \sigma_{\mathrm{SM}} + \sigma_{\mathrm{D8}} + \sigma_{\mathrm{int}}$ with the leading order SM cross section σ_{SM}, the dimension-eight term cross section σ_{D8} and the interference term cross section σ_{int}.

Although the dimension-six operators do not induce aNTGC at the tree-level, they can have an effect at the one-loop level. The one-loop contributions from dimension-six operators would be of the order of $(\alpha/4\pi)(\hat{s}/\Lambda^2)$

while the tree-level contribution from the dimension-eight operators are of the order of $(\hat{s}v^2/\Lambda^4)$ [1]. As a result, the contribution of the dimension-eight operators dominates the one-loop contribution of the dimension-six operators for $\Lambda \lesssim 2v\sqrt{\pi/\alpha} \approx 10$ TeV.

We have studied anomalous neutral triple gauge boson couplings from dimension-eight operators via the $pp \to l^+l^-\gamma$ process at High Luminosity Large Hadron Collider (HL-LHC) with 14 TeV center-of-mass energy, and we expect an enhancement due to the existence of aNTGCs with high-p_{T} photon in the final state [2–4]. The HL-LHC may provide a portal to complete opportunities at the LHC for discovery of new physics beyond the SM. The HL-LHC program as a top priority in particle physics in the context of developing the strategy for particle physics [5, 6] is planned at two benchmark values of integrated luminosity: the 300 fb^{-1} expected by the end of Run 3, and the 3 ab^{-1} expected to be delivered by the HL-LHC [7].

2. Cross sections

The leading order Feynman diagrams corresponding to the process $pp \to l^+l^-\gamma$ are given in Fig. 1. In this figure, the first diagram contains the anomalous $Z\gamma\gamma$ and $ZZ\gamma$ couplings, and second diagram contains only the anomalous $Z\gamma\gamma$ couplings, while the others come from SM electroweak processes. The operators in Eqs. (2)–(5) are implemented through FeynRules package [8] as a Universal FeynRules Output (UFO) [9]. After implementa-

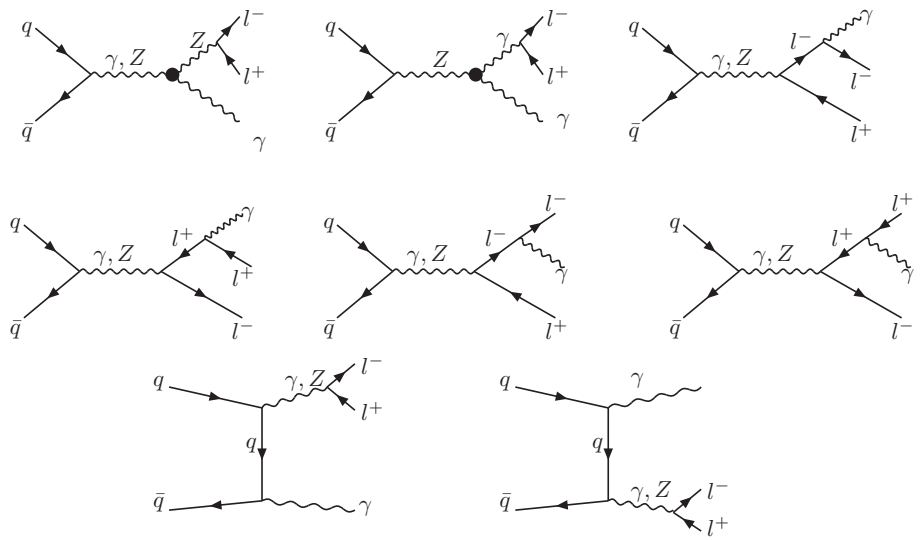

Fig. 1. Feynman diagrams for subprocess $q\bar{q} \to l^-l^+\gamma$ contributed from anomalous $Z\gamma\gamma$ and $Z\gamma Z$ vertices (first two) and the SM.

tion of this UFO model file, the cross section of $pp \to l^+l^-\gamma$ process at the center-of-mass energy of 14 TeV is calculated with MadGraph5_aMC@NLO [10]. In the study, we focus on CP-even $C_{\tilde{B}W}$ coupling and CP-odd C_{BB} coupling because the deviation in cross section from its SM value for these couplings is larger than that for C_{BW}, C_{WW} as mentioned in Ref. [11]. Figure 2 shows the cross sections of the $pp \to l^+l^-\gamma$ process as a function of two dimension-eight couplings $C_{\tilde{B}W}$, C_{BB}.

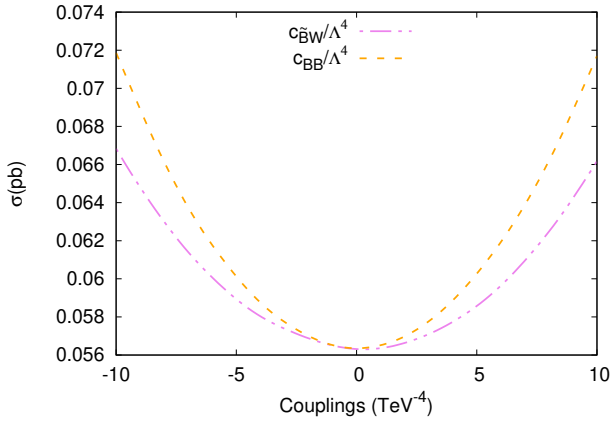

Fig. 2. The signal cross sections for the $pp \to l^-l^+\gamma$ process, with photon transverse momentum $p_{\mathrm{T}}^{\gamma} > 100$ GeV, depending on dimension-eight couplings at the HL-LHC.

For the kinematical distributions of leptons and photon in the $pp \to l^+l^-\gamma$ process, a minimum cut (generator level) for charged lepton and photon transverse momentum $p_{\mathrm{T}}^{l,\gamma} > 10$ GeV and pseudo-rapidity $|\eta_{l,\gamma}| < 2.5$ have been applied. In order to get better sensitivity to the couplings, we also generate the signal and background events with $p_{\mathrm{T}}^{\gamma} > 100$ GeV. For the event selection and analysis, we require angular separation $(\Delta R(l,\gamma) = \left[(\Delta\phi_{l,\gamma})^2 + (\Delta\eta_{l,\gamma})^2\right]^{1/2})$ between charged lepton and photon in the pseudo-rapidity-azimuthal angle plane. Basic cuts for the analysis are given as follows: (a) charged lepton transverse momentum $p_{\mathrm{T}}^{l} > 10$ GeV and pseudorapidity $|\eta^l| < 2.5$; (b) photon transverse momentum $p_{\mathrm{T}}^{\gamma} > 100$ GeV and photon pseudorapidity $|\eta^\gamma| < 2.5$; (c) charged lepton–photon separation $\Delta R(l,\gamma) > 0.7$; (d) the invariant mass of final-state charged leptons $m_{ll} > 50$ GeV.

3. Analysis framework

The study on effective dimension-eight aNTG couplings $C_{\tilde{B}W}$, C_{BB} and SM contribution as well as interference between effective couplings and SM

contributions have been performed via $pp \to l^+l^-\gamma$ process, where $l^\pm = e^\pm, \mu^\pm$. For the detailed analysis, we follow steps as shown in Fig. 3. The signal and background events are generated with MadGraph5_aMC@NLO and passed through the PYTHIA 6 [12] for parton showering and hadronization. The detector effects are included by ATLAS detector card in Delphes 3.3.3 [13] package. Then, all events are analyzed with ROOT [14] by using the ExRootAnalysis utility [15].

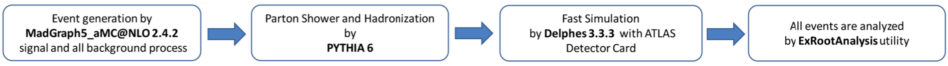

Fig. 3. A brief view of analysis flowchart chain.

For the event selection, we require one photon and at least two charged leptons ($l^\pm = e^\pm, \mu^\pm$); the same flavor but opposite sign and the angular separation between lepton and photon $\Delta R(l, \gamma) > 0.7$. The transverse momentum distribution of photon (in the final state of process $pp \to l^+l^-\gamma$) is shown in Fig. 4 (left panel). The invariant mass distributions of the $l^+l^-\gamma$ system are shown in Fig. 4 (right panel). The deviations from SM background at large values of $p_{\mathrm{T}}^{\gamma} \gtrsim 200$ GeV and $m_{ll\gamma} \gtrsim 500$ GeV become more pronounced. Therefore, we impose the following cuts in addition to the above-mentioned initial cuts: (a) $p_{\mathrm{T}}^{\gamma} > 400$ GeV, (b) $m_{ll\gamma} > 500$ GeV and (c) $m_{ll} > 50$ GeV in order to separate signal from the SM background efficiently. Figure 5 shows $\cos\theta_l^*$ distributions of signal for $C_{\tilde{B}W}/\Lambda^4$ (left panel), C_{BB}/Λ^4 (right panel) couplings and SM background. Here, $\cos\theta_l^*$ is the polar angle in the l^+l^- rest frame with respect to the l^+l^- direction in the $l^+l^-\gamma$ rest frame. Since the angular distribution of final-state par-

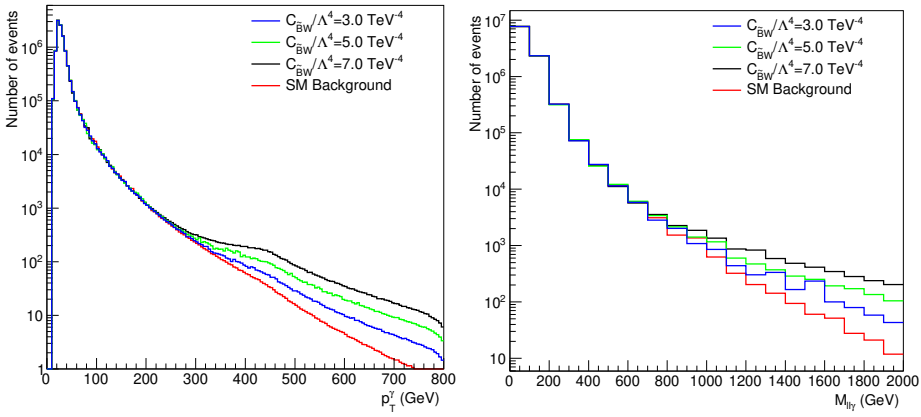

Fig. 4. The transverse momentum distribution of photon p_{T}^{γ} (left) and the invariant mass distribution $M_{ll\gamma}$ (right) for three different values of coupling $C_{\tilde{B}W}/\Lambda^4$ and SM background of $pp \to l^-l^+\gamma$ process.

ticles from signal and background processes is different, we have used this distribution as a tool to obtain attainable limits on effective dimension-eight aNTG couplings. Distributions given in Fig. 4 and Fig. 5 are normalized to the number of expected events which is defined to be the cross section of each processes times integrated luminosity of $L_{\text{int}} = 3000\ \text{fb}^{-1}$.

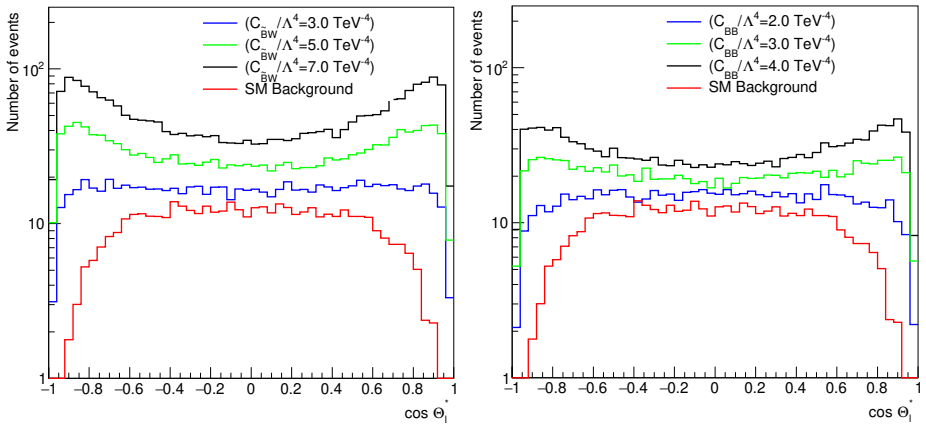

Fig. 5. The $\cos\theta_l^*$ distributions for $C_{\tilde{B}W}/\Lambda^4$ (left panel) and C_{BB}/Λ^4 (right panel) and SM background of the $pp \to l^-l^+\gamma$ process.

In order to obtain 95% C.L. limits on the aNTG couplings, a χ^2 criterion with and without systematic error is applied. Here, χ^2 function is defined as follows:

$$\chi^2 = \sum_i^{n_{\text{bins}}} \left(\frac{N_i^{\text{NP}} - N_i^{\text{B}}}{N_i^{\text{B}} \Delta_i} \right)^2 , \tag{7}$$

where N_i^{NP} is the total number of events in the existence of effective couplings, N_i^{B} is total number of events of the corresponding SM backgrounds in i^{th} bin of the $\cos\theta_l^*$ distributions, $\Delta_i = \sqrt{\delta_{\text{sys}}^2 + 1/N_i^{\text{B}}}$ is the combined systematic (δ_{sys}) and statistical errors in each bin. Applying these analysis cuts, we find the number of background events as 460 for $L_{\text{int}} = 3\ \text{ab}^{-1}$. The one-parameter χ^2 results of signal events obtained from $\cos\theta_l^*$ distributions for $C_{\tilde{B}W}/\Lambda^4 = 3.0, 5.0, 7.0\ \text{TeV}^{-4}$ and $C_{BB}/\Lambda^4 = 2.0, 3.0, 4.0\ \text{TeV}^{-4}$ are given in Tables I and II, respectively. In these tables, a cut on the photon transverse momentum $p_{\text{T}}^{\gamma} > 400$ GeV and integrated luminosity of $3\ \text{ab}^{-1}$ are considered, while only one coupling at a time is varied from its SM value. The two-dimensional 95% C.L. intervals in planes of $C_{\tilde{B}W}/\Lambda^4$ and C_{BB}/Λ^4 are presented in Fig. 6. One can also find one-dimensional confidence intervals on the relevant parameter axes.

TABLE I

The number of signal events and χ^2 results for various coupling value of $C_{\tilde{B}W}/\Lambda^4$ after applied kinematic cuts presented in the text using $\cos\theta_l^*$ distributions of the $pp \to l^- l^+ \gamma$ process with $L_{\rm int} = 3$ ab^{-1}.

$C_{\tilde{B}W}/\Lambda^4$ [TeV^{-4}]	Number of events	χ^2 $\delta_{\rm sys} = 0$	χ^2 $\delta_{\rm sys} = 3\%$	χ^2 $\delta_{\rm sys} = 5\%$
3.0	811	269.02	190.31	125.20
5.0	1458	2171.40	1536.12	1010.53
7.0	2464	8743.88	6185.72	4069.24

TABLE II

The number of signal events and χ^2 results for various coupling value of C_{BB}/Λ^4 after applied kinematic cuts presented in the text using $\cos\theta_l^*$ distributions of the $pp \to l^- l^+ \gamma$ process with $L_{\rm int} = 3$ ab^{-1}.

C_{BB}/Λ^4 [TeV^{-4}]	Number of events	χ^2 $\delta_{\rm sys} = 0$	χ^2 $\delta_{\rm sys} = 3\%$	χ^2 $\delta_{\rm sys} = 5\%$
2.0	695	120.71	85.40	39.41
3.0	1037	726.09	513.66	337.91
4.0	1464	2199.84	1556.24	1023.77

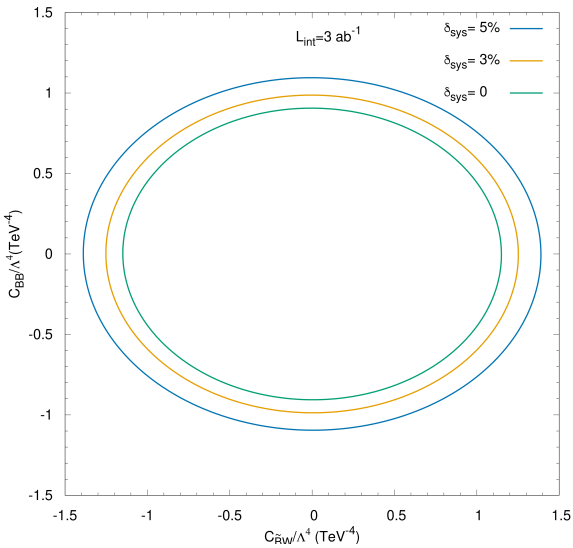

Fig. 6. Two-dimensional 95% C.L. intervals in planes of $C_{\tilde{B}W}/\Lambda^4$ and C_{BB}/Λ^4.

4. Discussion and conclusion

The effects of dimension-eight operators in $Z\gamma\gamma$ and $Z\gamma Z$ vertices are investigated via the $pp \to l^-l^+\gamma$ process. Both the final-state photon transverse momentum (p_{T}^{γ}) and polar angle ($\cos\theta_l^{\star}$) are considered as a discriminant to extract bounds for $C_{\tilde{B}W}/\Lambda^4$ and C_{BB}/Λ^4 couplings. Our expected limits on dimension-eight aNTG couplings at 95% C.L. for the HL-LHC with $L_{\mathrm{int}} = 300$ fb^{-1} and 3000 fb^{-1} are given in Table III as $[-1.88 : 1.88]$ TeV^{-4} and $[-1.14; 1.14]$ TeV^{-4} for $C_{\tilde{B}W}/\Lambda^4$, and the limits are $[-1.47 : 1.47]$ TeV^{-4} and $[-0.86; 0.86]$ TeV^{-4} for C_{BB}/Λ^4 (where $p_{\mathrm{T}}^{\gamma} > 400$ GeV applied), respectively. The 95% C.L. current limits on dimension-eight operators converted from coefficients of dimension-six operators for the process $pp \to ZZ \to l^+l^-l'^+l'^-$ at $\sqrt{s} = 13$ TeV and $L_{\mathrm{int}} = 36.1$ fb^{-1} from the ATLAS Collaboration are reported as -5.9 TeV$^{-4} < C_{\tilde{B}W}/\Lambda^4 < 5.9$ TeV^{-4} and -2.7 TeV$^{-4} < C_{BB}/\Lambda^4 < 2.8$ TeV^{-4} [16]. Comparing with the current experimental results, we obtain 5 and 3 times better sensitivity for dimension-eight couplings $C_{\tilde{B}W}/\Lambda^4$ and C_{BB}/Λ^4 , respectively. We conclude that the limits on aNTG couplings would be improved from the HL-LHC results once the systematic uncertainties are kept under control.

TABLE III

Obtained limits on $C_{\tilde{B}W}/\Lambda^4$ and C_{BB}/Λ^4 at 95% C.L. with $L_{\mathrm{int}} = 300$ fb^{-1} and 3 ab^{-1} by assuming a non-zero dimension-eight operator at a time for the $pp \to l^-l^+\gamma$ process.

Couplings	$L_{\mathrm{int}} = 300$ fb^{-1}			$L_{\mathrm{int}} = 3$ ab^{-1}		
[TeV^{-4}]	$\delta_{\mathrm{sys}} = 0$	$\delta_{\mathrm{sys}} = 3\%$	$\delta_{\mathrm{sys}} = 5\%$	$\delta_{\mathrm{sys}} = 0$	$\delta_{\mathrm{sys}} = 3\%$	$\delta_{\mathrm{sys}} = 5\%$
$C_{\tilde{B}W}/\Lambda^4$	[−1.88:1.88]	[−1.89:1.89]	[−1.92:1.92]	[−1.14:1.14]	[−1.22:1.22]	[−1.34:1.34]
C_{BB}/Λ^4	[−1.47:1.47]	[−1.49:1.49]	[−1.51:1.51]	[−0.86:0.86]	[−0.93:0.93]	[−1.02:1.02]

Authors' work was partially supported by the Turkish Atomic Energy Authority (TAEK) under the project grant No. 2018TAEK (CERN) A5.H6.F2-20.

REFERENCES

[1] C. Degrande, *J. High Energy Phys.* **1402**, 101 (2014) [arXiv:1308.6323 [hep-ph]].

[2] V.D. Barger, H. Baer, K. Hagiwara, *Phys. Rev. D* **30**, 1513 (1984).

[3] U. Baur, E.L. Berger, *Phys. Rev. D* **47**, 4889 (1993).

[4] U. Baur, T. Han, J. Ohnemus, *Phys. Rev. D* **57**, 2823 (1998) [arXiv:hep-ph/9710416].

[5] ATLAS Collaboration, ATL-PHYS-PUB-2012-001, ATL-COM-PHYS-2012-1118.

[6] ATLAS Collaboration, ATL-PHYS-PUB-2012-004, ATL-COM-PHYS-2012-1455.

[7] ATLAS Collaboration, arXiv:1307.7292 [hep-ex].

[8] A. Alloul *et al.*, *Comput. Phys. Commun.* **185**, 2250 (2014) [arXiv:1310.1921 [hep-ph]].

[9] C. Degrande *et al.*, *Comput. Phys. Commun.* **183**, 1201 (2012) [arXiv:1108.2040 [hep-ph]].

[10] J. Alwall *et al.*, *J. High Energy Phys.* **1407**, 079 (2014) [arXiv:1405.0301 [hep-ph]].

[11] A. Senol *et al.*, *Nucl. Phys. B* **935**, 365 (2018).

[12] T. Sjöstrand, S. Mrenna, P.Z. Skands, *J. High Energy Phys.* **0605**, 026 (2006) [arXiv:hep-ph/0603175].

[13] J. de Favereau *et al.* [DELPHES 3 Collaboration], *J. High Energy Phys.* **1402**, 057 (2014) [arXiv:1307.6346 [hep-ex]].

[14] R. Brun, F. Rademakers, *Nucl. Instrum. Methods Phys. Res. A* **389**, 81 (1997).

[15] P. Demin, https://cp3.irmp.ucl.ac.be/projects/ExRootAnalysis/wiki/UserManual

[16] M. Aaboud *et al.* [ATLAS Collaboration], *Phys. Rev. D* **97**, 032005 (2018) [arXiv:1709.07703 [hep-ex]].